Cell, Vol. 104, 71–81, January 12, 2001, Copyright ©2001 by Cell Press

Complexins Regulate a Late Step in Ca^{2+}-Dependent Neurotransmitter Release

Kerstin Reim,*# Michael Mansour,†# Frederique Varoqueaux,* Harvey T. McMahon,‡‖ Thomas C. Südhof,‡ Nils Brose,*§ and Christian Rosenmund†§

*Max-Planck-Institut für Experimentelle Medizin
Abteilung Neurogenetik
AG Molekulare Neurobiologie
Hermann-Rein-Str. 3
D-37075 Göttingen
Bundesrepublik Deutschland

†Max-Planck-Institut für Biophysikalische Chemie
Abteilung Membranbiophysik
Am Faßberg 11
D-37077 Göttingen
Bundesrepublik Deutschland

‡University of Texas Southwestern Medical Center
Center for Basic Neuroscience
Department of Molecular Genetics and
Howard Hughes Medical Institute
6000 Harry Hines Boulevard
Dallas, Texas 75235

Summary

Synaptic vesicle fusion at synapses is triggered by increases in cytosolic Ca^{2+} levels. However, the identity of the Ca^{2+} sensor and the transduction mechanism of the Ca^{2+} trigger are unknown. We show that Complexins, stoichiometric components of the exocytotic core complex, are important regulators of transmitter release at a step immediately preceding vesicle fusion. Neurons lacking Complexins show a dramatically reduced transmitter release efficiency due to decreased Ca^{2+} sensitivity of the synaptic secretion process. Analyses of mutant neurons demonstrate that Complexins are acting at or following the Ca^{2+}-triggering step of fast synchronous transmitter release by regulating the exocytotic Ca^{2+} sensor, its interaction with the core complex fusion machinery, or the efficiency of the fusion apparatus itself.

Introduction

Synaptic neurotransmitter release is mediated by the exocytotic fusion of synaptic vesicles with a specialized presynaptic plasma membrane region at the active zone. Typically, a subpopulation of vesicles is tethered specifically to the active zone plasma membrane. These tethered vesicles have to be primed to fusion competence before their fusion can be triggered by rises in the intracellular Ca^{2+} concentration. Usually, only a fraction of tethered vesicles in any given synapse is primed and ready to fuse in response to the Ca^{2+} trigger. The size of this so-called readily releasable vesicle pool determines synaptic release probability and signaling capacity (Zucker, 1996).

The molecular mechanisms that mediate the active zone processes of vesicle priming and Ca^{2+} triggered fusion are now beginning to emerge (Südhof, 1995; Calakos and Scheller, 1999; Jahn and Südhof, 1999). Several studies demonstrated that the active zone protein Munc13-1 functions as an essential synaptic vesicle priming factor (Brose et al., 2000). Vesicle fusion, on the other hand, is thought to be mediated by the concerted action of the synaptic vesicle protein Synaptobrevin/VAMP (vesicle associated membrane protein) and the two synaptic plasma membrane proteins Syntaxin and SNAP25 (synaptosomal associated protein of 25 kDa). These proteins form a thermodynamically stable ternary complex, the core complex, whose association is thought to represent the primed state of a vesicle and/or to mediate vesicle fusion (Calakos and Scheller, 1999; Jahn and Südhof, 1999). Munc13-1 may mediate its priming effect by modulating Syntaxin function, thereby promoting core complex formation at the active zone (Brose et al., 2000). The best candidates for the exocytotic Ca^{2+} sensor are the synaptic vesicle protein Synaptotagmin I and related proteins (Geppert and Südhof, 1998).

In a search for proteins that act downstream of Munc13-1-mediated synaptic vesicle priming, we found recently that levels of Complexin I (CPX I) were significantly reduced in Munc13-1 deletion mutants. This indicated an altered half-life of this protein in the Munc13-1 mutant background (Augustin et al., 1999b), suggesting that CPX I may act downstream of Munc13-1-mediated vesicle priming, e.g., in Ca^{2+} triggered fusion.

In mammals, CPXs form a family of two closely related proteins (CPX I and II) that were initially identified as stoichiometric components of the core complex (Ishizuka et al., 1995; McMahon et al., 1995; Takahashi et al., 1995). There is no evidence for additional CPX isoforms in current human genome databases. CPXs are small (15–16 kDa), polar, soluble proteins that bind to assembled core complexes and compete with α-SNAP (soluble NSF attachment protein) for binding (McMahon et al., 1995). CPXs are enriched in synapses (Takahashi et al., 1995; Ono et al., 1998; Yamada et al., 1999) where they are present in soluble and insoluble pools. Studies involving overexpression/microinjection of protein or microinjection of antibodies suggested that CPXs may function as negative regulators of neurotransmitter release (Ono et al., 1998; Itakura et al., 1999). However, deletion of CPX II in mice results in a phenotype with almost entirely normal synaptic physiology (Takahashi et al., 1999).

In the present study, we use double deletion mutant mice to demonstrate that CPXs are important positive regulators of synaptic vesicle exocytosis. Our data sug-

§To whom correspondence should be addressed (e-mail: crosenm@gwdg.de or brose@em.mpg.de).
‖Present address: MRC Laboratory of Molecular Biology, Neurobiology Division, Hills Road, Cambridge CB2 2QH, United Kingdom.
#These authors contributed equally to this work.

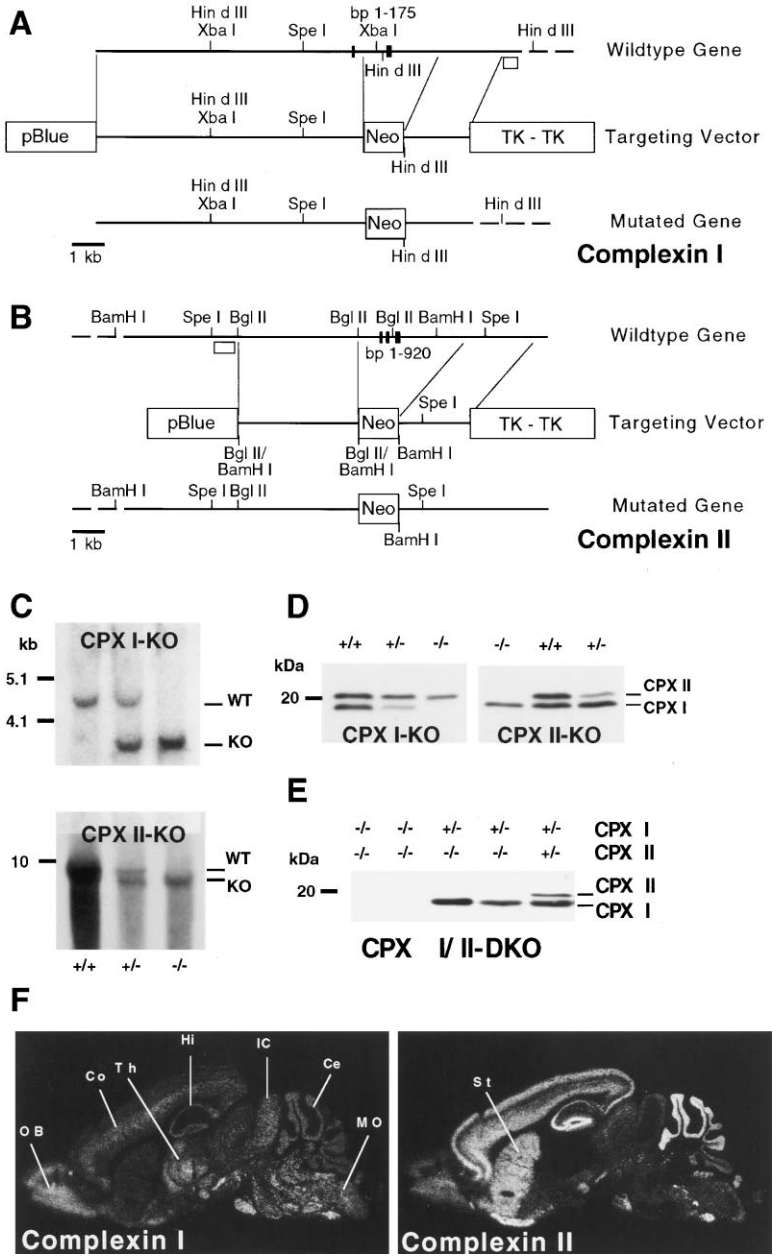

Figure 1. Mutation of Murine CPX Genes

(A and B) Deletion of CPX I (A) and CPX II (B) in the mouse. Maps of the wild-type *CPX I* and *CPX II* genes, the respective targeting vectors, and the resulting mutant genes are shown. Positions of exons (black boxes with bp of corresponding cDNA) and restriction enzyme sites are indicated. The position of probes used to identify mutant alleles are indicated by open bars. Neo, neomycin resistance gene; TK, thymidine kinase gene.

(C) Southern blot analyses of single deletion mutations in mice. Mouse tail DNA from adult wild-type mice (+/+), and mice heterozygous (+/−) or homozygous (−/−) for the mutation in the *CPX I* or *CPX II* genes were analyzed as described in Experimental Procedures. Positions of wild-type (WT) and mutant (KO) alleles are indicated.

(D) CPX expression in CPX I or CPX II single deletion mutant mice. Left, CPX I mutation. Right, CPX II mutation. Brain homogenates (20 μg protein per lane) from adult wild-type (+/+), heterozygous (+/−), and homozygous (−/−) mutant mice were analyzed by SDS-PAGE and immunoblotting using an anti-CPX I/II antibody. Positions of CPX I and CPX II protein are indicated.

(E) CPX expression in CPX I/II double deletion mutant mice generated by two double heterozygous parents. Brains from newborn littermates of the indicated genotypes (in this litter only heterozygous (+/−) and homozygous (−/−) mutants) were analyzed by SDS-PAGE and immunoblotting using an anti-CPX I/II antibody.

(F) Expression of CPX I and II mRNA in mouse brain. Negative X-ray film images showing the distribution of CPXs I (left) and II (right) in sagittal sections of the whole adult mouse brain. Negative controls with excess unlabeled oligonucleotides were devoid of signal. Ce, Cerebellum; Co, cerebral cortex; Hi, hippocampus; IC, inferior colliculus; MO, medulla oblongata; OB, olfactory bulb; St, striatum; Th, thalamus.

gest that CPXs function at or following the Ca^{2+}-triggering step of neurotransmitter release.

Results

Generation of CPX I and CPX II Deletion Mutant Mice

Deletion mutations in the murine *CPX I* and *II* genes and homozygous single and double mutants with their respective controls were generated as described in Experimental Procedures (Figures 1A and 1B).

Southern blot analysis of offspring resulting from interbreeding of mice heterozygous for the CPX I or CPX II mutation demonstrated that the respective genotypes (wild-type +/+, heterozygous +/−, homozygous −/−; Figure 1C) were present at the expected Mendelian frequency. Western blot analysis of brains from adult animals showed that protein expression was completely abolished in the respective homozygous mutants while protein levels in heterozygous animals were reduced (Figure 1D). Double mutants lacking both CPXs were generated by interbreeding of parents carrying at least one mutant allele of each *CPX* gene. For routine experimentation, mice heterozygous for the CPX I mutation and homozygous for the CPX II mutation were crossed to obtain double mutant offspring and control littermates with two wild-type *CPX I* alleles. Again, the respective genotypes (CPX I +/+, +/−, or −/−, CPX II −/−) were obtained at the expected Mendelian frequency. Standard Western blot analysis of brains from newborn pups obtained in such interbreedings showed that expression of CPX I and CPX II is abolished in homozygous double mutants (Figure 1E).

In principle, the targeting strategy for the *CPX I* gene

allows for the generation of truncated CPX I forms due to the use of alternative translational start sites (e.g., Met^{16} or Met^{19}). However, no such truncated forms were detectable in the mature hippocampal cultures (10 days in vitro) that were used for all our studies.

Basic Characteristics of CPX I and CPX II Deletion Mutant Mice

We found that mice lacking CPX II show no obvious phenotypic changes. In contrast, homozygous CPX I deletion mutants develop a strong ataxia, suffer from sporadic seizures, are unable to reproduce, and die within 2–4 months after birth. Although loss of CPX I is ultimately fatal, the fact that mice lacking either CPX I or CPX II live for at least 2 months after birth indicates that CPXs I and II are partially redundant. We therefore generated double mutants lacking both CPX isoforms. Homozygous CPX I/II double mutants die within a few hours after birth.

In order to detect possible developmental changes or alterations in brain structure due to CPX deletion mutations, we analyzed morphological characteristics of brains from homozygous adult CPX I and CPX II single mutants as well as newborn CPX I/II double mutants. We found that in all cases, the structure and cytoarchitecture of mutant brains and the distribution of synaptic markers (Synaptophysin, vesicular GABA-transporter VGAT) are very similar to the respective control (not shown). In a search for changes in the protein composition of mutant synapses, we analyzed the levels of selected synaptic proteins in mutant and control brains. The expression levels of all tested synaptic proteins were found to be unaffected in the three different types of homozygous mutants. Tested proteins included (I) α-SNAP, CPX II, Munc13-1, Munc13-2, Munc13-3, Munc18-1, NSF (N-ethylmaleimide-sensitive fusion protein), SNAP25, Synapsin I/IIa, Synapsin IIb, Synaptobrevin 2, Synaptophysin, Synaptotagmin 1, Syntaxin 1, and VGAT in the case of CPX I mutants; (II) α-SNAP, CPX I, Munc13-1, Munc13-2, Munc13-3, Munc18-1, SNAP25, Synapsin I/IIa, Synapsin IIb, Synaptobrevin 2, Synaptophysin, Synaptotagmin 1, and Syntaxin 1 in the case of CPX II mutants; and (III) SNAP25, Synaptobrevin 2, Synaptotagmin 1, Syntaxin 1, and VGAT in the case of the CPX I/II double mutants (not shown).

These data indicate that individual CPX isoforms are partially dispensable while loss of both known CPX isoforms causes death of newborn mutants. Because CPXs are presynaptic proteins that interact with components of the transmitter release machinery (Ishizuka et al., 1995; McMahon et al., 1995; Takahashi et al., 1995; Ono et al., 1998; Yamada et al., 1999), and because no morphological changes in brain cytoarchitecture were observed in homozygous single and double mutants, the most likely explanation for the lethality of the CPX I/II double deletion is a compromised synaptic function. To analyze synaptic deficits in mice lacking CPXs, we studied the functional and structural characteristics of synapses between mutant neurons.

Functional and Structural Characteristics of Synapses in CPX I/II Double Mutant Mice

Evoked Neurotransmitter Release

We concentrated our analysis of synapse structure and function in CPX mutants on CPX I/II double mutant mice. These exhibited the most pronounced phenotypic alterations of all CPX mutant genotypes, most likely owing to partial redundancy.

In the case of perinatally lethal phenotypes, characteristics of synaptic transmission are best and most reliably studied in primary cultures. One frequently used culture system is the hippocampal autaptic microdot culture. We therefore tested in initial in situ hybridization experiments whether the two CPX isoforms are expressed in mouse hippocampus. We found that both CPXs are coexpressed in many regions of the brain (Figure 1F). Most importantly, pyramidal cells in the CA regions of the hippocampus as well as granule cells in the dentate gyrus were found to express both CPX I and II. Differential distributions of the two CPXs were apparent in parts of the thalamus (no CPX II), the striatum (no/little CPX I), and in superficial layers of the cerebral cortex (no/little CPX I). Thus, the mouse hippocampal primary culture system is well suited for the analysis of CPX I/II double mutants.

Patch clamp recordings from single isolated neurons were used to assess possible defects of presynaptic properties induced by the loss of CPXs. Synaptic responses were evoked by brief somatic depolarization (2 ms depolarization from -70 mV holding potential to 0 mV) and measured as peak inward currents a few ms after action potential induction. We concentrated our analysis on glutamatergic neurons, as they are much more abundant than inhibitory GABAergic cells in autaptic cultures. EPSC amplitudes recorded from homozygous CPX I and CPX II single mutant neurons were indistinguishable from those measured in cells of corresponding wild-type littermates (Figure 2B). Because in these and all following experiments CPX II-deficient cells were essentially identical to wild-type controls, we used homozygous CPX II single mutant littermates as controls in our analysis of homozygous CPX I/II double mutants. This approach facilitated the production of double mutants and respective control animals at sufficient frequencies in the same litters. In contrast to mutations in individual CPX genes, CPX I/II double mutant cells exhibited a 66% reduction in EPSC amplitudes when compared to their control littermates (Figures 2A and 2B). Comparison between wild-type groups ($p = 0.94$) or between CPX II groups ($p = 0.37$) from the different interbreedings revealed no significant differences. Thus, double deletion of CPXs I and II leads to a strong reduction in evoked EPSC amplitudes in comparison to wild-type and single CPX mutant controls.

To exclude that the reduced amplitude in CPX I/II double mutant cells resulted from an impaired capacity to form synapses, we quantified synapse densities using immunohistochemical markers. Cultures were double stained with antibodies to the presynaptic marker Synaptophysin and the dendritic marker MAP-2 (microtubule associated protein), and the number of synapses per 10 μm dendrite was counted. Irrespective of the genotype, neurons were found to generate similar numbers of synapses (Figure 2C), indicating that lack of CPXs does not interfere with synaptogenesis in culture. We therefore concentrated our subsequent analysis on changes in synaptic physiology as the most likely cause for the mutant phenotype. In particular, we searched for changes in postsynaptic sensitivity, vesicular transmitter load, sizes of readily releasable vesicle pools and

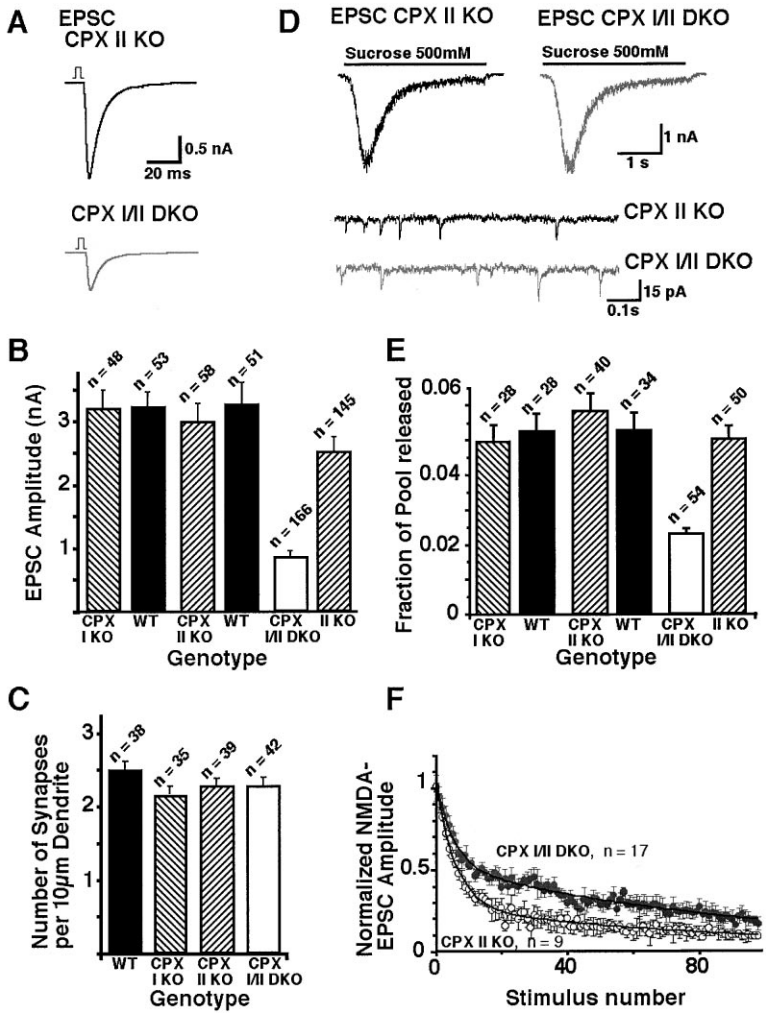

Figure 2. Synaptic Amplitudes, Readily Releasable Vesicle Pools, Spontaneous Release, and Synaptic Release Probability in Glutamatergic CPX I Single Mutant, CPX II Single Mutant, and CPX I/II Double Mutant Neurons

(A) Raw traces showing autaptic EPSCs from a CPX I/II double mutant (bottom) and a CPX II single mutant neuron (top). The somatic current was blanked for display purposes.

(B) Bar diagram summarizing average synaptic EPSC amplitudes for CPX I mutants compared to their wild-type littermates (from three mice each), CPX II mutants compared to their wild-type littermates (ten and nine mice, respectively) and CPX I/II double mutants compared to CPX II single mutant littermates (ten and eleven mice, respectively). Values of n indicate number of cells.

(C) Synapse densities in cultures of the indicated genotypes. Hippocampal neuronal cultures were double stained with primary antibodies to synaptophysin and MAP-2. Error bars indicate standard error of the mean, and n represents the total number of evaluated dendrites (data are from cultures of two wild-type [511 synapses], CPX II single mutant [449 synapses], and CPX I/II double mutant mice [463 synapses], and from three independent CPX I single mutant mice [393 synapses]).

(D) Representative raw traces of responses to hypertonic solution from CPX II single mutant and CPX I/II double mutant neurons (top). Hypertonic solution was applied for 4 s as indicated by the black bar. Genotypes as in (A).

(E) Bar diagram showing the average vesicular release probability of neurons of the indicated genotypes. Values of n indicate number of cells.

(F) Analysis of MK-801 blocking rate in CPX II single mutant (n = 9) and CPX I/II double mutant neurons (n = 17) revealing reduced synaptic release probability in CPX I/II double mutant cells. The average NMDA EPSC amplitude normalized to the first response in the presence of MK-801 (5 μM) is plotted against evoked EPSC stimulus number. The decay of the amplitudes of CPX II single mutant cells (empty circles) as well as of CPX I/II double mutant cells (gray filled circles) were fitted with two exponentials. The amplitude of the fast decay component was significantly reduced in the CPX I/II double mutant cells.

vesicular release probability as possible reasons for the reduced EPSCs of mutant neurons.

Spontaneous Neurotransmitter Release

We examined mEPSC amplitude and charge in order to detect possible changes in postsynaptic responsiveness or vesicular transmitter load as a consequence of the CPX I/II double deletion. Spontaneous activity was measured at −70 mV in the presence of 200 nM tetrodotoxin. We found that mEPSC frequencies, amplitudes, and charges were essentially identical in all genotypes tested (Table 1). Thus, we can rule out that a vesicular transmitter uptake process or a postsynaptic dysfunction is responsible for the reduced evoked EPSC amplitudes observed in CPX I/II double mutants. Rather, the observed phenotype is likely to be due to a compromised regulation of the presynaptic transmitter release machinery.

Readily Releasable Vesicle Pools and Release Probability

In principle, changes in any step of the synaptic vesicle cycle can ultimately influence evoked EPSC sizes. In a first attempt to identify the step in the synaptic vesicle cycle that is affected by the loss of CPX I/II, we performed a detailed analysis of the sizes of readily releasable vesicle pools in neurons of the different CPX mutant genotypes. The fact that the mEPSC rates were not significantly different between the different genotypes (Table 1) already suggested that the size of the readily releasable vesicle pool is not changed in the absence of CPXs. Sizes of readily releasable vesicle pools were quantified by measuring the responses of mutant cells and their appropriate controls to application of 500 mOsm hypertonic sucrose solution for 3–4 s. Typically, this treatment induces release of the readily releasable vesicle pool, which in turn leads to a transient inward current followed by a steady current component (Rosenmund and Stevens, 1996; Figure 2D). The transient part consists of a burst-like release of vesicles resulting from the forced fusion of all fusion-competent, primed vesicles. The total number of vesicles in the readily releasable pool of a cell is represented by the integral of the total charge of the transient current component after

Table 1. Summary of Pool-, mEPSC-, and Evoked Release Parameters

Genotype	n	mEPSC Amplitude (pA)	mEPSC Charge (fC)	mEPSC Rate (Hz)	Readily Releasable Pool (10^3 vesicles)	Refilling Rate (Pool-units • s^{-1})
CPX I KO	28	20.1 ± 1.6	100 ± 1	5.3 ± 0.6	6.10 ± 1.2	0.17 ± 0.013
WT I	28	21.3 ± 0.7	103 ± 4	5.5 ± 0.6	6.35 ± 0.9	0.14 ± 0.014
CPX II KO	48	21.1 ± 0.8	104 ± 3	7.2 ± 0.9	6.09 ± 0.7	0.14 ± 0.014
WT II	34	21.5 ± 0.9	101 ± 4	7.1 ± 0.8	5.73 ± 0.8	0.13 ± 0.016
CPXI/II DKO	54	22.8 ± 0.4	104 ± 3	5.9 ± 0.7	6.08 ± 0.8	0.15 ± 0.014
CPX II KO	50	23.1 ± 1.1	110 ± 4	6.9 ± 0.7	5.92 ± 0.7	0.14 ± 0.013

Parameters were calculated from cells in which data for synaptic responses, pool size, mEPSC charge, and mEPSC frequency were obtained in parallel. In cases where no mEPSC data were obtained, translation of pool parameters into number of vesicles was based on the average mEPSC charge of the respective genotype. mEPSC charge, amplitude, and frequency measurements were obtained from at least 200 events in 19–28 cells per genotype.

application of hypertonic solution divided by the charge of the average mEPSC. In all analyzed genotypes, the vesicle pool size was similar and amounted to approximately 6000 vesicles per cell (Figure 2D; Table 1). Direct comparison of mEPSC rates and pool sizes showed that the spontaneous fusion rate of individual vesicles was unchanged in all groups and that total readily releasable pools were completely turned over within approximately 800 s (not shown). Thus, the reduced evoked EPSC amplitudes in neurons lacking CPXs I and II are not due to an underlying reduction of readily releasable vesicle pools.

The sustained component of the postsynaptic current induced by hypertonic sucrose solutions provides a measure for the refilling rate of the readily releasable vesicle pool. The refilling rate, in turn, is a measure for the efficiency of synaptic vesicle translocation, docking, and priming at the active zone. We estimated the refilling rate of the readily releasable pool by linear approximation of the sustained release rate during hypertonic sucrose stimulation. Similar refilling rates (0.13–0.17 s^{-1}) for all examined genotypes were observed (Table 1), demonstrating that vesicle translocation, docking, and priming rates are not affected by CPX I/II loss.

Above results strongly suggest that neurons lacking CPXs I and II are perfectly capable of translocating, docking, and priming of synaptic vesicles, whose intrinsic ability to fuse spontaneously is entirely normal. Consequently, the observed reduction of evoked EPSC amplitudes in CPX I/II double mutants must be caused at a step in the synaptic vesicle cycle that follows vesicle priming but most likely precedes the fusion reaction itself. Thus, the synaptic neurotransmitter release deficiency observed in CPX I/II double mutants most likely represents a defective coupling of transmitter release to the action potential, e.g., at the Ca^{2+}-triggering step. A direct measure for the efficiency of action potential induced vesicle release is the vesicular release probability P_{vr}. We determined P_{vr} by dividing the number of vesicles released during an action potential through the number of vesicles in the readily releasable vesicle pool. We found that P_{vr} was 5%–6% in cells from all control genotypes (i.e., wild-type, CPX I −/−, CPX II −/−), but only 2.4% in CPX I/II double mutant cells (Figure 2E). This reduction in the transmitter release efficiency from CPX I/II double mutant neurons was similarly apparent when peak release rates were used as an alternative measure (not shown).

The synaptic release probability P_r depends on the number of fusion competent vesicles per synapse and their release probability P_{vr}. Thus, the reduction in vesicular release probability P_{vr} that we observed in CPX I/II double mutant neurons (Figure 2E, Table 1) should result in a reduced synaptic release probability P_r. We estimated the synaptic release probability in double mutant mice by analyzing the progressive block of NMDA receptor-mediated synaptic currents in the presence of MK-801, which reflects the release probability across all synapses of a given neuron (Rosenmund et al., 1993). Both, CPX I/II double mutant neurons and control cells showed the typical amplitude decay in the presence of MK-801 with two time constants (Figure 2F). Further analysis of synaptic release probability distribution predicted a 49% reduction of synaptic amplitudes for double mutant cells in comparison to CPX II single mutant controls. This is in excellent agreement with amplitude ratios observed under the conditions of MK-801 measurements (48 ± 5%, n = 6, at 2.7 mM Ca^{2+}, no added Mg^{2+}), demonstrating that the reduction of vesicular release probability P_{vr} in CPX I/II double mutant neurons results in a concomitant reduction of synaptic release probabilities P_r.

So far, our analysis of mutant neurons suggested a role for CPXs in a very late step of vesicle exocytosis that follows vesicle priming. To examine whether the ultrastructural morphology of double mutant synapses is compatible with this idea, we performed an electron microscopic analysis of cultures from CPX I/II double mutants and CPX II single mutant controls. As with our electrophysiological studies, we focused in our ultrastructural analysis on glutamatergic, asymmetric Type 1 synapses. We found that neurons of both genotypes form typical Type 1 synapses with distinct postsynaptic densities and presynaptic vesicle clusters (Figures 3A and 3B). A detailed morphometric analysis demonstrated that CPX I/II double deficient synapses (n = 145) are indistinguishable from CPX II single mutant controls (n = 36). Most importantly, the sizes of active zones (193 ± 9 and 208 ± 28 nm for double mutants and controls, respectively; $p > 0.5$), the density of vesicles within 150 nm of the active zone (317 ± 7 and 312 ± 14 per μm^2 for double mutants and controls, respectively; $p > 0.4$), and the number of docked vesicles at active zones (17.4 ± 0.7 and 18.3 ± 1.0 per μm active zone in double mutant and controls, respectively; $p > 0.4$) were not significantly different between the two

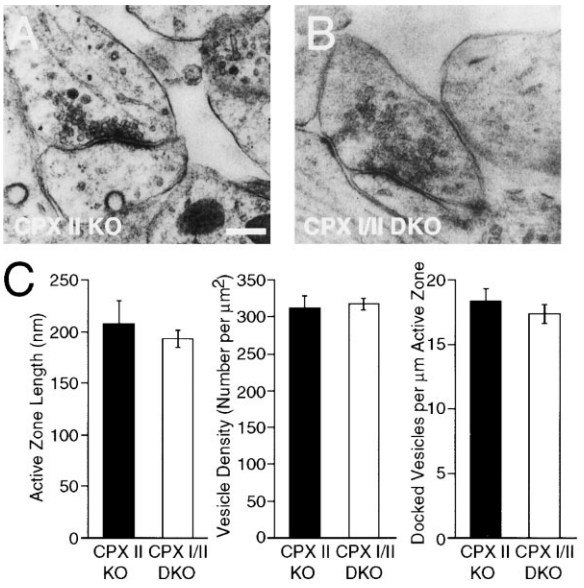

Figure 3. Ultrastructural Characteristics of Synapses in CPX I/II Double Mutant Mice

(A and B) Micrographs of sections through CPX II single mutant (+/+, −/−; A) synapses, which were used as controls, as well as CPX I/II double mutant (−/−, −/−; B) synapses (20,000-fold magnification). Scale bar: 200 nm.

(C) Bar diagrams expressing the active zone length, vesicle density within a 150 nm range of the active zone, and number of docked vesicles per μm active zone in control (n = 36 synapses from cultures of three independent animals) and CPX I/II double mutant synapses (n = 145 synapses from cultures of four independent animals). No significant differences were observed between the two genotypes ($p > 0.4$ in all analyses). Only asymmetric synapses were analyzed. Error bars indicate standard error.

tested genotypes (Figure 3C). These findings exclude the possibility that developmental or morphological changes contribute to the CPX I/II double mutant phenotype. They are compatible with the idea that deletion of both CPXs disturbs the synaptic vesicle cycle after the vesicle priming step because in this case, no striking ultrastructural changes would be expected (Augustin et al., 1999b).

Short Term Plasticity

Changes in the synaptic release probability of a neuron cause concomitant changes in short term plasticity of synaptic transmission. Trains of action potentials lead to facilitation in synapses with low initial release probability, but to depression in synapses with high initial release probability. We measured synaptic amplitudes from CPX I/II double mutant neurons and CPX II single mutant control cells during trains of action potentials at stimulation frequencies of 10 Hz (Figure 4A). CPX II single mutant control cells showed a progressive depression of EPSC amplitudes. In contrast, EPSC amplitudes in double mutant cells increased during the first few stimuli and reached control levels by the fifth stimulus. Similar results were obtained during 20 Hz (not shown) and 50 Hz stimulation of evoked release (five pulses, Figure 4B). This facilitation of transmitter release from double mutant cells correlates well with the fact that initial synaptic release probability is reduced in these mutant neurons.

Interestingly, we also observed in our 50 Hz stimulation experiments that the slow, asynchronous component of release from double mutant cells following the 50 Hz train tended to be at least as large as or even larger than that in control cells (Figure 4B). This suggests that CPXs selectively affect fast synchronous neurotransmitter release, as has been reported for Synaptotagmin I (Geppert et al., 1994). To determine whether this specific effect of the CPX I/II double mutation on synchronous transmitter release is independent of stimulation history, we reanalyzed the time course of evoked EPSCs during low frequency stimulation. We averaged EPSCs from double mutant and control cells and examined the time course of release (Figure 4C). Peak release rates were normalized to the size of the readily releasable vesicle pool and were found to be three times larger in CPX II single mutant control cells (4.82 pool units/s) than in CPX I/II double mutant cells (1.70 pool units/s). Synchronous release was distinguished from asynchronous release by exponential fitting of the evoked charge integral (Figure 4C). We observed a striking and selective difference between double mutant and control cells with respect to the level of synchronous transmitter release. In double mutant cells, only 1.5 ± 0.2% of the total releasable pool was released during the synchronous release phase while the corresponding value in control cells was 4.1 ± 0.3% (Figure 4D). In contrast, the relative contribution of asynchronous release (1.1% of the releasable pool; Figure 4D) and the time constants of the synchronous and asynchronous release processes as determined in the fits were similar in double mutant and control cells. Thus, lack of CPXs I and II causes a selective reduction of the synchronous release component.

Ca^{2+} Sensitivity of Evoked Transmitter Release

So far, our analyses allow the conclusion that lack of CPXs I and II results in a postpriming defect, causing a reduced efficiency of synchronous evoked neurotransmitter release. The consequences of this defect cease with ongoing release evoked at high frequencies. Together with the following observations, above conclusions suggest a role for CPXs in the direct or indirect control of the Ca^{2+} sensitivity of transmitter release: (I) Once vesicles in CPX I/II double mutant cells reach a fusion competent state, they can be released upon elevation of the intracellular Ca^{2+} concentration; (II) during ongoing high frequency activity, Ca^{2+} concentrations in the terminal seem to rise sufficiently to overcome the CPX I/II mutant phenotype; (III) the initially reduced vesicular release probability together with the pronounced paired-pulse facilitation in CPX I/II double mutant cells resembles wild-type synapse behavior at lowered extracellular Ca^{2+} concentrations; (IV) like deletion of CPXs I and II, loss of Synaptotagmin I, a putative Ca^{2+} sensor in neurotransmitter release, leads to a specific inhibition of synchronous release (Geppert et al., 1994).

To test the possibility that CPX I/II deficiency causes a decrease in the apparent Ca^{2+} sensitivity of the release machinery, we measured evoked EPSC amplitudes in double mutant and control cells as a function of the external Ca^{2+} concentration $[Ca^{2+}]_o$. EPSC amplitudes were evoked at 0.2 Hz for a period of 45 s at Ca^{2+} concentrations of 0.5–20 mM, while the Mg^{2+} concentration was left constant at 1 mM. To standardize the re-

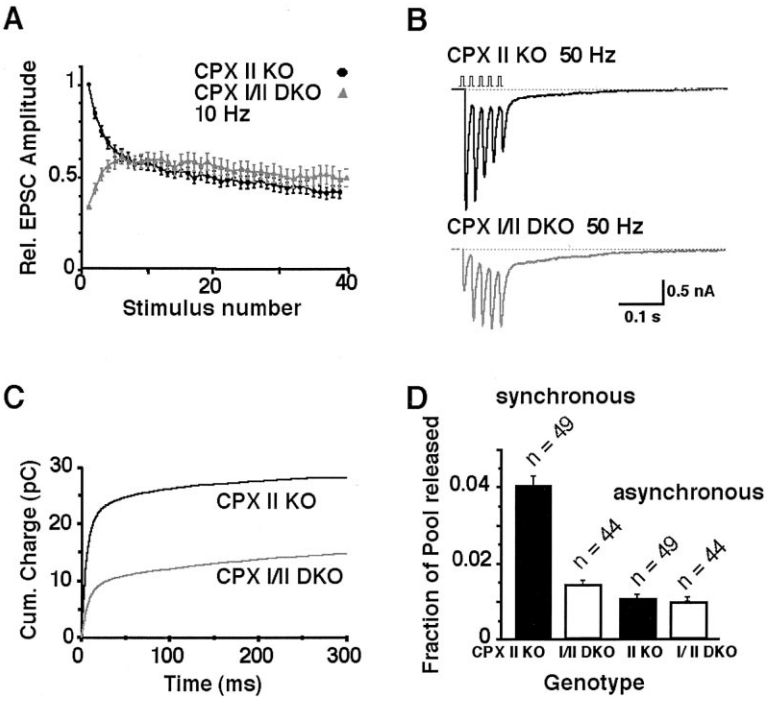

Figure 4. Release During High Frequency Stimulation, Synchronous and Asynchronous Synaptic Release in CPX I/II Double Mutant Neurons

(A) Average peak amplitudes (normalized to the average initial amplitude in control cells) of EPSCs evoked at 10 Hz frequency. Note that control cells from CPX II single mutants (n = 27) show depression while CPX I/II double mutant cells (n = 31) show facilitation. With the fifth stimulus, peak amplitudes reached similar absolute levels.

(B) Average synaptic responses of CPX II single mutant (n = 50) and CPX I/II double mutant neurons (n = 50) during five EPSCs evoked at an interpulse interval of 20 ms. Note that the CPX I/II double mutant responses show strong amplitude facilitation and that the total release was at least as large as in the CPX II mutants due to a pronounced asynchronous current component. This current component was blocked by NBQX (10 μM) and not affected by AP-5 (25 μM).

(C) Integral of averaged absolute synaptic responses of CPX I/II double mutant (n = 50) and CPX II single mutant neurons (n = 45). Double exponential fit (not shown) of the current integral was used to distinguish two (defined as synchronous, τ = 6.2–7.5 ms, and asynchronous, τ = 125–185 ms) kinetic phases of release. Note the reduced synchronous release component for the CPX I/II double mutant response, while the absolute slow component is unchanged.

(D) Summary of the synchronous and asynchronous EPSC component for CPX II single mutant and CPX I/II double mutant cells expressed as a fraction of the pool released per action potential.

sponses between cells and to control for rundown of synaptic responses, individual test measurements were preceded and followed by EPSC measurements under standard conditions (4 mM $[Ca^{2+}]_o$ /4 mM $[Mg^{2+}]_o$). The response at each Ca^{2+} concentration was normalized to the response at the standard concentration. To compare the Ca^{2+} dose response curves between CPX I/II double mutant and control cells, we scaled the dose response curve of double mutant cells to control cells according to the absolute synaptic EPSC amplitudes under standard conditions. Cells of both genotypes responded to increases in extracellular Ca^{2+} concentrations with increases in evoked EPSC amplitudes (Figure 5A). However, the Ca^{2+} dose response curves were clearly different between CPX I/II double mutant and control cells (Figure 5B). As we suspected that the synchronous release phase is selectively affected by the loss of CPXs, we separately measured the Ca^{2+} sensitivity of both the synchronous and asynchronous release phase. Three important observations were made in this analysis. First, amplitudes of asynchronous release were indistinguishable between the tested genotypes over the entire range of Ca^{2+} concentrations tested, indicating that the asynchronous release phase is not dependent on the presence of CPXs (Figure 5B). Using standard Hill function fitting, the apparent K_D values for asynchronous release for CPX I/II double mutant and CPX II single mutant control cells were found to be 6.0 ± 1.8 and 7.7 ± 1.6 mM Ca^{2+}, respectively. Second, the apparent K_D values for the synchronous release phase was clearly shifted to the right in double mutant cells, amounting to 6.8 ± 1.5 mM and 3.4 ± 0.4 mM Ca^{2+} for CPX I/II double mutant and CPX II single mutant control cells, respectively (Figure 5B). Third, maximal values of synchronous release measured at the highest Ca^{2+} concentrations tested were found to be similar between CPX I/II double mutant and CPX II single mutant control cells (Figure 5B), and maximum values predicted by the fit were identical (45.2 ± 2.6 pC versus 45.3 ± 6 pC). Thus, the apparent Ca^{2+} sensitivity of synchronous transmitter release in CPX I/II double mutant cells is significantly reduced. This impairment can be fully rescued by high Ca^{2+} concentrations.

In view of the fact that CPXs interact with the exocytotic core complex, the decreased Ca^{2+} sensitivity of transmitter release in CPX I/II double mutant cells is most likely due to changes in the Ca^{2+}-triggering step of exocytosis at the level of core complex function or its interaction with the Ca^{2+} sensor. Alternatively, loss of CPXs I and II could affect Ca^{2+} channel density, localization, or function, thereby causing reductions in the amplitudes of Ca^{2+} transients during an action potential. Although the latter possibility is unlikely because the Ca^{2+} sensor of asynchronous release is apparently unaffected by loss of CPXs I and II (Figure 5B), we tried to distinguish between the two possible causes of altered Ca^{2+} sensitivity by inducing Ca^{2+}-dependent release independently of Ca^{2+} channels. We monitored spontaneous EPSC activity induced by elevations of intracellular Ca^{2+} concentrations in response to the Ca^{2+} ionophore Calcimycin. Although Calcimycin-induced release is inherently asynchronous, we assumed that distinct synchronously and asynchronously releasable vesicle pools exist in neurons, and that the majority of vesicles re-

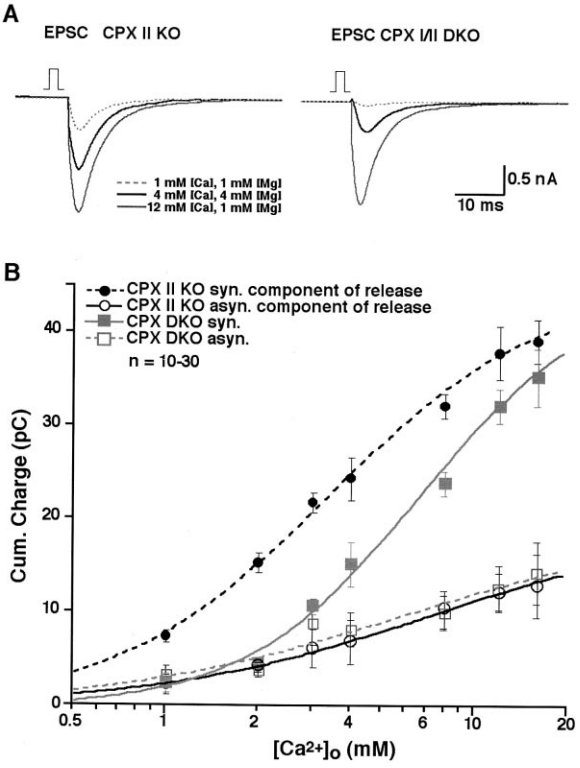

Figure 5. Dependency of Synchronous and Asynchronous Release upon External Ca^{2+}

(A) Raw traces of EPSCs from a CPX II single mutant (left) and a CPX I/II double mutant neuron (right) recorded in 1 mM Ca^{2+}/1 mM Mg^{2+}, 12 mM Ca^{2+}/1 mM Mg^{2+}, and under control conditions (4 mM Ca^{2+}, 4 mM Mg^{2+}).

(B) $[Ca^{2+}]_o$ dose response curve and Hill fits for average absolute synchronous and asynchronous release, normalized to the response under control conditions.

leased by Calcimycin treatment originate from pools that, during evoked responses, would be released in a synchronous fashion. Calcimycin was applied at 10 μM for 100 s, and spontaneous EPSCs were recorded (Figure 6A). In addition, evoked EPSCs were measured at 3 s intervals throughout the period of ionophore treatment (Figure 6C). Calcimycin treatment of control cells led to a transient and massive increase of spontaneous EPSC activity that exhibited an onset time constant of 13 s, reached a peak amplitude (measured as NBQX-sensitive inward current) of 495 ± 83 pA (n = 29; four animals) after approximately 20 s, and returned to baseline activity with a time constant of 20 s (Figure 6B). In contrast, double mutant cells showed a more delayed spontaneous EPSC activity (onset time constant 19.2 s, peak time 33 s, decay time constant 39.4 s) with only a moderate peak release activity of 225 ± 18 pA (n = 32; three animals) (Figure 6B). Thus, release from CPX I/II double mutant cells remains less sensitive to Ca^{2+} even when Ca^{2+} channels are bypassed with Calcimycin, indicating that changes in Ca^{2+} channel density, localization, or function are unlikely to contribute to the CPX I/II double mutant phenotype. In addition, the data show that CPX I/II deficiency indeed alters the apparent Ca^{2+} sensitivity of exocytosis, possibly by affecting the Ca^{2+} sensing step or its transduction into fusion. Interestingly, the total Ca^{2+}-dependent release activity induced over the entire period of Calcimycin treatment (100 s) was not different between double mutant and control cells (20.1 ± 2.4 versus 21.8 ± 2.5 pool units turned over during 100 s), suggesting that release reaches control levels once Ca^{2+} concentrations have risen sufficiently high (see also release during prolonged 10 Hz trains, Figure 4A).

The conclusion that CPX I/II deficiency indeed affects the apparent Ca^{2+} sensitivity of transmitter release was further supported by our analysis of evoked EPSCs during Calcimycin treatment (Figure 6C). In control cells, evoked EPSC amplitudes exhibited a short phase of subtle augmentation, followed by progressive reduction of the synaptic response, presumably due to depletion of the readily releasable pool of vesicles. In contrast, double mutant neurons showed a delayed but much more pronounced augmentation of evoked EPSC amplitudes. This observation reflects the fact that double mutant cells start off with reduced EPSC amplitudes that facilitate as the intracellular Ca^{2+} concentration rises. Thus, Calcimycin treatment mimics high frequency stimulation (Figures 4A and 4B). In both cases, intracellular Ca^{2+} concentrations build up, eventually leading to an unusually pronounced facilitation of release from double mutant neurons.

Discussion

In contrast to previously published studies on CPX function involving more indirect assays (Ono et al., 1998; Itakura et al., 1999), the present study shows that CPXs are late acting positive regulators of transmitter secretion. Mice lacking both CPXs die immediately after birth. Double mutant neurons exhibit normal readily releasable vesicle pool sizes (Figure 2D, Table 1) and spontaneous transmitter release characteristics (Table 1), but their vesicular and synaptic release probabilities in response to action potentials are dramatically reduced (Figures 2E and 2F). The mutant phenotype is specific for the fast synchronous Ca^{2+} triggered release phase (Figures 4C and 4D) and can be rescued completely by increasing the extracellular Ca^{2+} concentration, indicating a 50% decrease in the apparent sensitivity of the release machinery to Ca^{2+} (Figure 5B). The mutant phenotype is still detectable when Ca^{2+} channels are bypassed by an ionophore, suggesting that changes at the level of Ca^{2+} entry through voltage gated channels (e.g., changes in function, density, distribution, or physical coupling to the secretion apparatus) do not contribute to the phenotypic alterations in CPX-deficient neurons (Figure 6). The fact that increases in the extracellular Ca^{2+} concentration can rescue the mutant phenotype (Figure 5B) indicates that the exocytotic machinery can still function with normal V_{max} provided that sufficiently high intracellular Ca^{2+} levels are reached. Thus, although not essential for the maintenance of a residual release activity, CPXs are essential for survival of the organism.

Changes in the presynaptic Ca^{2+} buffering capacity (assuming that CPXs act as anti-buffers) or in Ca^{2+} transport and sequestration are unlikely to be causally involved in the deletion mutant phenotype because the Ca^{2+} sensitivity of the asynchronous release phase is

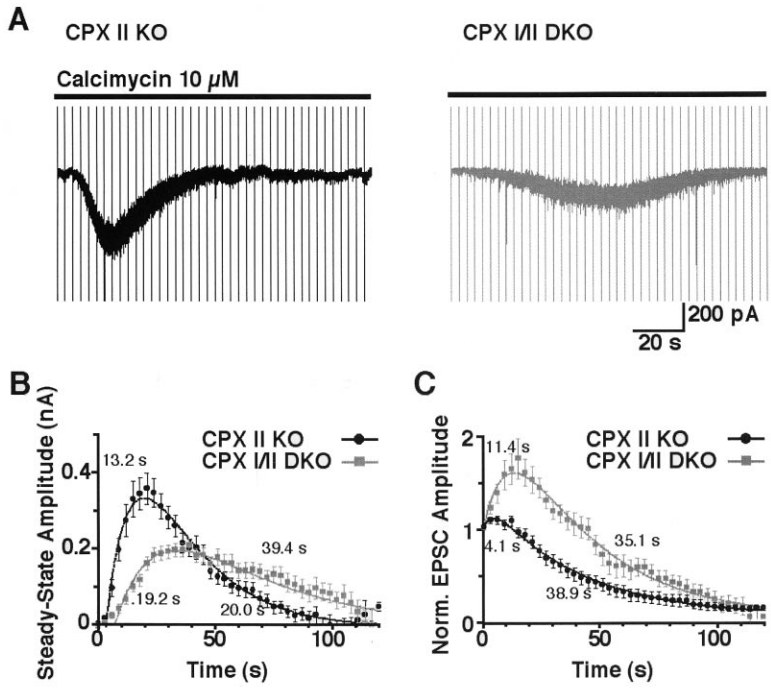

Figure 6. Release Induced by a Calcium-Ionophore

(A) During Calcimycin (10 μM) application (black bar), spontaneous EPSC rates and evoked release were monitored. Representative raw current traces of CPX II single mutant (left) and CPX I/II double mutant cells (right) are shown. Vertical lines at 3 s intervals represent stimulation artifacts resulting from intermittent monitoring of EPSCs. Calcimycin-induced Ca^{2+} elevation led to a decreased and slowed release rate of spontaneous Ca^{2+}-dependent vesicle release in the double mutant neurons relative to CPX II single mutant cells.

(B) Average time course of sEPSC activity as measured by the NBQX-dependent inward current (n = 29 cells from four mice and n = 32 cells from three mice for CPX II single and CPX I/II double mutants, respectively). The values next to the average traces indicate rise and decay time constants from biexponential fits (dotted lines).

(C) Average normalized time course of evoked EPSC amplitudes during Calcimycin application (n = 29 cells from four mice and n = 32 cells from three mice for CPX II single and CPX I/II double mutants, respectively). Time courses were fitted with two exponentials to determine onset and decay time constants (values indicated).

unaffected by the mutation while the Ca^{2+} sensitivity of the synchronous release phase is specifically reduced (Figure 5B). Moreover, overexpression of CPXs in chromaffin cells has very little effect on Ca^{2+} triggered secretion (J. Rettig, personal communication). Finally, a role of CPXs as Ca^{2+} anti-buffers or regulators of Ca^{2+} transport and sequestration is not compatible with current biochemical views of CPX function (Pabst et al., 2000). Taken together, our observations are best compatible with an enhancer role of CPXs in the Ca^{2+}-triggering event or a subsequent step of synaptic vesicle fusion.

The transduction mechanism by which rises in intracellular Ca^{2+} concentrations elicit synaptic vesicle fusion is unknown. In response to Ca^{2+} influx, an exocytotic Ca^{2+} sensor is thought to increase the release probability of readily releasable vesicles that can otherwise exocytose spontaneously with only a very low probability. The as yet unidentified Ca^{2+} sensor is thought to function after initial core complex assembly, that is after vesicle priming and partial completion of the fusion reaction (e.g., to stalk-like hemifusion). At the molecular level, the activated sensor in the Ca^{2+}-loaded state may trigger full fusion of primed vesicles by acting upon assembled core complexes in the trans state or by inducing membrane bilayer perturbations through phospholipid binding (Südhof and Rizo, 1996; Davis et al., 1999). Alternatively, the core complex itself could serve as a Ca^{2+} sensor (Sutton et al., 1998).

The fact that CPX loss leads to a fatal reduction in the apparent Ca^{2+} sensitivity of transmitter release can be explained by at least four different models.

First, CPXs could be the Ca^{2+} sensors themselves. We regard this possibility as unlikely because the deletion mutant phenotype can be overcome by increased extracellular Ca^{2+} concentrations. Assuming that no other CPX is expressed in brain and that no unknown mechanisms limit synaptic transmission and lead to an approximation of control and double mutant responses at high Ca^{2+} concentrations, this observation suggests that a sensor other than CPXs is still functional in double mutant neurons. In the absence of CPXs, the sensor can still trigger secretion at normal V_{max} in the presence of sufficiently high Ca^{2+} concentrations, but the apparent Ca^{2+} sensitivity of secretion is reduced.

Second, CPXs could increase the affinity or association rates, or decrease dissociation rates of the Ca^{2+} sensor. This model implies that CPXs serve as some sort of coreceptors that interact directly or indirectly with the Ca^{2+} sensor. Compatible with the data presented in the present study, the absence of CPXs would then lead to a reduced affinity of the sensor for Ca^{2+}. Such a scenario would be particularly attractive if core complexes themselves were the exocytotic Ca^{2+} sensors because CPXs bind to assembled core complexes in a 1:1 stoichiometry (McMahon et al., 1995; Pabst et al., 2000).

Third, CPXs could facilitate the interaction between the fusion machinery and the Ca^{2+} sensor in its Ca^{2+} bound state. This model implies that maximal release activity can be achieved with only a fraction of Ca^{2+} sensors being activated. The model would predict that CPXs increase the affinity of core complexes, the most likely sensor target, toward the Ca^{2+} bound sensor. In the absence of CPXs, less core complexes would be binding to the sensor at Ca^{2+} concentrations that are usually sufficient to trigger release, resulting in the observed decrease in the apparent Ca^{2+} sensitivity of secretion. In order to reach wild-type levels of transmitter release in CPX I/II double mutants, unusually high Ca^{2+} levels would be necessary to generate higher concentra-

tions of activated sensor molecules. This in turn would overcome the reduced affinity of the core complex toward the activated Ca^{2+} sensor and lead to wild-type like secretion rates (Figure 5). Again, this scenario is nicely compatible with the fact that CPXs bind to assembled core complexes, the putative target of sensor action, in a 1:1 stoichiometry (McMahon et al., 1995; Pabst et al., 2000).

Fourth, CPXs could act in the process following Ca^{2+} sensor interaction with the fusion machinery by enhancing the efficiency of the fusion reaction itself. This model assumes that each primed vesicle carries multiple primed fusion or core complexes in the trans state and that maximal fusion rates are achieved with only a defined fraction of fusion complexes per vesicle being activated. In agreement with our data, it predicts that loss of CPXs leads to less efficient fusion at Ca^{2+} concentrations that are usually sufficient to trigger release. This mutant phenotype could be overcome by increased presynaptic Ca^{2+} concentrations (see Figure 5) as these would activate more Ca^{2+} sensors/fusion complexes. One caveat with this model is that CPXs do not appear to affect core complex assembly and disassembly in vitro (Pabst et al., 2000).

Very similar to the consequences of CPX I/II double deletion mutations are the effects of nerve cell poisoning with certain Chlostridial neurotoxins that proteolytically cleave core complex components (BoNT A and, to a lesser extent, BoNT E, but not tetanus toxin, BoNT B, and BoNT D). Treatment with BoNT A, which cleaves SNAP25, leads to a reduction of evoked transmitter release that can be reversed by elevated Ca^{2+} concentrations (see Gerona et al., 2000 for a recent account and discussion of the classical literature). Together with the finding that SNAP25 interacts with Synaptotagmin in a Ca^{2+}-dependent and BoNT A sensitive manner (Gerona et al., 2000), the characteristics of BoNT A effects indicate that perturbances of core complex function or of core complex interactions with putative Ca^{2+} sensors result in changes of the apparent Ca^{2+} sensitivity of transmitter release, essentially supporting the last two of our models of CPX function described above.

Our study demonstrates that CPXs are important, late acting regulators of synaptic vesicle fusion. Clearly, further information is needed in order to determine the molecular mechanism of CPX action. In particular, the identity of the exocytotic Ca^{2+} sensor needs to be elucidated before our suggested models can be distinguished unequivocally. In the meantime, current Ca^{2+} sensor candidates (e.g., Synaptotagmins) can be tested with respect to the models presented above.

Experimental Procedures

In Situ Hybridization

In situ hybridization experiments were performed as described (Augustin et al., 1999a). Antisense oligonucleotides representing the following sequences were chosen as probes: bp 34–78 of CPX I cDNA (GenBank accession number NM_007756) and bp 50–94 of CPX II cDNA (GenBank accession number NM_009946).

Stem Cell Experiments

CPX I and CPX II mutant mice were generated by homologous recombination in embryonic stem cells as described (Thomas and Capecchi, 1987; Augustin et al., 1999b). To generate the CPX I targeting vector (Figure 1A), two genomic clones (pBlueMG-CPX10A and pBlueMG-CPXI 10B) containing two exons (one with part of the 5′ untranslated region and the first coding exon) were used. In the targeting vector, the first coding exon of the *CPX I* gene (representing bp 72–175 of the CPX I cDNA, GenBank accession number NM_007756) was replaced by a neomycin resistance cassette. In the case of CPX II (Figure 1B), clone pBlueMG-CPX3 containing three coding exons was used. In the targeting vector, all three exons (representing bp 1–920, i.e., the complete coding sequence, of the CPX II cDNA, GenBank accession number NM_009946) were replaced by the neomycine resistance cassette. Following electroporation and selection, recombinant stem cell clones were analyzed by Southern blotting (Figure 1C) after digestion of DNA with HindIII (CPX I) and BamHI (CPX II). For hybridization, outside probes localized 3′ of the targeting vector short arm (CPX I) or 5′ of the targeting vector long arm (CPX II) were used. Two positive clones of each genotype were injected into mouse blastocysts to obtain highly chimeric mice that transmitted the mutation through the germline. Germline transmission of the mutations was confirmed by Southern blotting (genomic DNA) and immunoblotting (brain extracts). Subsequently, genotyping was performed by PCR. Because mice homozygous for the CPX I mutation are atactic, it was not possible to use them for further breeding. To obtain CPX I/II double mutant mice, animals heterozygous for the CPX I mutation and homozygous for the CPX II mutation were crossed. For all experiments, homozygous mutants were compared with appropriate control littermates. For the analysis of CPX I and CPX II single deletion mutants, wild-type and homozygous mutant littermates were obtained by interbreeding of heterozygous mutant parents. In all morphological and electrophysiological analyses of hippocampal neurons, single deletion mutants of either CPX I or CPX II were indistinguishable from their wild-type littermates (see Results). Therefore, CPX I/II double mutants were obtained by interbreeding of mice homozygous for the CPX II mutation and heterozygous for the CPX I mutation, and compared to homozygous CPX II mutant mice that carried two wild-type alleles of the *CPX I* gene.

Immunoblotting

Immunoblotting analyses of brains from newborn CPX I/II double mutants and newborn control mice (CPX I +/+, CPX II −/−) as well as of brains from adult CPX I and CPX II single mutants and their respective wild-type control littermates were done as described (Augustin et al., 1999b). Antibodies to the following proteins were used: α-SNAP, CPX I/II, Munc13-1, Munc13-2, Munc13-3, Munc18-1, NSF, SNAP25, Synapsin I/IIa, Synapsin IIb, Synaptobrevin 2, Synaptophysin, Synaptotagmin 1, Syntaxin 1, and VGAT. All antibodies were from Synaptic Systems, except for antibodies to Munc-13 isoforms (Augustin et al., 1999a), and VGAT (S. Takamori, Göttingen).

Light and Electron Microscopy

Light microscopic determinations of synapse densities (number of Synaptophysin-positive presynaptic terminals per 10 μm MAP-2-positive dendrite) in neuronal cultures were done as described (Augustin et al., 1999b). Likewise, ultrastructural analyses of synapses were performed according to published procedures (Augustin et al., 1999b). Only asymmetric synapses with clearly identifiable postsynaptic densities were analyzed. We analyzed the size of the active zones, the density of vesicles within a 150 nm range of the active zone, and the number of docked vesicles (as defined by a direct contact between vesicles and plasma membrane) per μm active zone length. For both, light and electron microscopic analyses, number-coded photographs from mutant and control cultures were analyzed in a blind fashion.

Cell Culture and Electophysiology

Microisland cultures of mouse hippocampal neurons were prepared and maintained as described (Bekkers and Stevens, 1991; Rosenmund et al., 1993, 1995; Rosenmund and Stevens, 1996; Augustin et al., 1999b). Neurons were grown in a chemically defined medium (NBA+B27, Gibco). For each experiment, approximately equal numbers of cells from the respective genotypes were measured in parallel and blindly on the same day in vitro (10–16 days in vitro). The standard extracellular medium contained (mM): NaCl, 140; KCl, 2.4;

HEPES, 10; glucose, 10; $CaCl_2$, 4; $MgCl_2$, 4; 300 mOsm, pH 7.3. Sensitivity of synaptic responses to external Ca^{2+} was measured at constant Mg^{2+} concentrations (1 mM). NMDA-EPSCs were measured at 2.7 mM external Ca^{2+} in the presence of 10 μM glycine and in the absence of external Mg^{2+}. The release probability in wild-type neurons under these conditions is 1.3 times larger than under standard conditions (4 mM Ca^{2+}/4 mM Mg^{2+}). Hypertonic solution for pool size determination was made by adding 500 mM sucrose to the extracellular solution. Solutions were applied as described previously (Rosenmund et al., 1995). To examine synaptically activated currents, experiments were performed using recurrent synapses (autapses) on microisland cultures at room temperature (~24°C). To determine vesicular release probability, evoked responses and responses to hypertonic sucrose solutions were always recorded successively from the same cell. The number of readily releasable vesicles per cell was calculated by dividing the integrated transient burst component of the response to hypertonic sucrose solution by the average mEPSC charge measured in the same cell (if determined) or by the mean mEPSC charge averaged across cells. Detection of mEPSCs was usually performed for at least 60 s. Data were analyzed with a template detection program (Axograph 4.1). Threshold for detection was set to 3.5 times the baseline standard deviation. Captured mEPSCs of individual cells were averaged to determine mean amplitude and charge. These values were also used to normalize evoked release and pool size to the number of quanta released. Mean mEPSC rates and pool size determinations from individual cells were used to calculate the spontaneous release rate expressed as pool units/s. Peak quantal release rate was calculated by first dividing the charge integral of a single EPSC by the charge of the readily releasable pool (current integral of the sucrose response). This normalized trace was then differentiated with the y axis representing pool units/s or s^{-1}. Asynchronous and synchronous EPSC components were quantified by fitting the EPSC integral with two time constants. Patch clamp recordings were performed as described (Augustin et al., 1999b). D-5-Aminophophonovalerate (AP-5; 25–50 μM) was added in experiments examining high frequency stimulation, asynchronous release, and Ca^{2+} sensitivity. Data are expressed as mean ± standard error. Significance was tested using a nonparametric Mann-Whitney test.

Acknowledgments

We thank I. Herfort, S. Wenger, and T. Hellmann for excellent technical assistance and the staff of the animal core facility at the Max-Planck-Institut für Experimentelle Medizin for invaluable help with blastocyst injections and animal husbandry. We are grateful to S. Takamori and R. Jahn for antibodies and to D. Fasshauer, R. Fernandez-Chacon, R. Jahn, E. Neher, S. Pabst, and J. Rettig for helpful discussions. This work was funded by a joint grant (Ro1296/6-1) from the Deutsche Forschungsgemeinschaft to C. R. and N. B.; C. R. and N. B. are Heisenberg Fellows of the Deutsche Forschungsgemeinschaft.

Received July 17, 2000; revised November 27, 2000.

References

Augustin, I., Betz, A., Herrmann, C., Jo, T., and Brose, N. (1999a). Differential expression of two novel Munc13 proteins in rat brain. Biochem. J. *337*, 363–371.

Augustin, I., Rosenmund, C., Südhof, T.C., and Brose, N. (1999b). Munc13-1 is essential for fusion competence of glutamatergic synaptic vesicles. Nature *400*, 457–461.

Bekkers, J.M., and Stevens, C.F. (1991). Excitatory and inhibitory autaptic currents in isolated hippocampal neurons maintained in culture. Proc. Natl. Acad. Sci. USA *88*, 7834–7838.

Brose, N., Rosenmund, C., and Rettig, J. (2000). Regulation of transmitter release by Unc-13 and its homologues. Curr. Opin. Neurobiol. *10*, 303–311.

Calakos, N., and Scheller, R.H. (1999). Synaptic vesicle biogenesis, docking, and fusion: a molecular description. Annu. Rev. Physiol. *61*, 753–776.

Davis, A.F., Bai, J., Fasshauer, D., Wolowick, M.J., Lewis, J.L., and Chapman, E.R. (1999). Kinetics of synaptotagmin responses to Ca^{2+} and assembly with the core SNARE complex onto membranes. Neuron *24*, 363–376.

Geppert, M., and Südhof, T.C. (1998). Rab3 and synaptotagmin: The yin and yang of membrane fusion. Annu. Rev. Neurosci. *21*, 75–96.

Geppert, M., Goda, Y., Hammer, R.E., Li, C., Rosahl, T.W., Stevens, C.F., and Südhof, T.C. (1994). Synaptotagmin I: a major Ca^{2+} sensor for transmitter release at a central synapse. Cell *79*, 717–727.

Gerona, R.R.L., Larsen, E.C., Kowalchyk, J.A., and Martin, T.F.J. (2000). The C-terminus of SNAP25 is essential for Ca^{2+}-dependent binding of synaptotagmin to SNARE complexes. J. Biol. Chem. *275*, 6328–6336.

Ishizuka, T., Saisu, H., Odani, S., and Abe, T. (1995). Synaphin: A protein associated with the docking/fusion complex in presynaptic terminals. Biochem. Biophys. Res. Commun. *213*, 1107–1114.

Itakura, M., Misawa, H., Sekiguchi, M., Takahashi, S., and Takahashi, M. (1999). Transfection analysis of functional roles of CPX I and II in the exocytosis of two different types of secretory vesicles. Biochem. Biophys. Res. Commun. *265*, 691–696.

Jahn, R., and Südhof, T.C. (1999). Membrane fusion and exocytosis. Annu. Rev. Biochem. *68*, 863–911.

McMahon, H.T., Missler, M., Li, C., and Südhof, T.C. (1995). Complexins: cytosolic proteins that regulate SNAP receptor function. Cell *83*, 111–119.

Ono, S., Baux, G., Sekiguchi, M., Fossier, P., Morel, N.F., Nihonmatsu, I., Hirata, K., Awaji, T., Takahashi, S., and Takahashi, M. (1998). Regulatory roles of complexins in neurotransmitter release from mature presynaptic nerve terminals. Eur. J. Neurosci. *10*, 2143–2152.

Pabst, S., Hazzard, J.W., Antonin, W., Südhof, T.C., Jahn, R., Rizo, J., and Fasshauer, D. (2000). Selective interaction of Complexin with the neuronal SNARE complex. Determination of the binding regions. J. Biol. Chem., in press.

Rosenmund, C., Clements, J.D., and Westbrook, G.L. (1993). Nonuniform probability of glutamate release at a hippocampal synapse. Science *262*, 754–757.

Rosenmund, C., Feltz, A., and Westbrook, G.L. (1995). Synaptic NMDA receptor channels have a low open probability. J. Neurosci. *15*, 2788–2795.

Rosenmund, C., and Stevens, C.F. (1996). Definition of the readily releasable pool of vesicles at hippocampal synapses. Neuron *16*, 1197–1207.

Südhof, T.C. (1995). The synaptic vesicle cycle: A cascade of protein-protein interactions. Nature *375*, 645–653.

Südhof, T.C., and Rizo, J. (1996). Synaptotagmins, C_2-domain proteins that regulate membrane traffic. Neuron *17*, 379–388.

Sutton, R.B., Fasshauer, D., Jahn, R., and Brünger, A.T. (1998). Crystal structure of a SNARE complex involved in synaptic exocytosis at 2.4 Å resolution. Nature *395*, 347–353.

Takahashi, S., Yamamoto, H., Matsuda, Z., Ogawa, M., Yagyu, K., Taniguchi, T., Miyata, T., Kaba, H., Higuchi, T., Okutani, F., and Fujimoto, S. (1995). Identification of two highly homologous presynaptic proteins distinctly localized at the dendritic and somatic synapses. FEBS Lett. *368*, 455–460.

Takahashi, S., Ujihara, H., Huang, G.Z., Yagyu, K.I., Sanbo, M., Kaba, H., and Yagi, T. (1999). Reduced hippocampal LTP in mice lacking a presynaptic protein: complexin II. Eur. J. Neurosci. *11*, 2359–2366.

Thomas, K.R., and Capecchi, M.R. (1987). Site-directed mutagenesis by gene targeting in mouse embryo-derived stem cells. Cell *51*, 503–512.

Yamada, M., Saisu, H., Ishizuka, T., Takahashi, H., and Abe, T. (1999). Immunohistochemical distribution of the two isoforms of synaphin/complexin involved in neurotransmitter release: localization at the distinct central nervous system regions and synaptic types. Neuroscience *93*, 7–18.

Zucker, R.S. (1996). Exocytosis: a molecular and physiological perspective. Neuron *17*, 1049–1055.